Joint Distributed Beamforming and Power Allocation in Underlay Cognitive Two-Way Relay Links Using Second-Order Channel Statistics

Yun Cao and Chintha Tellambura, *Fellow, IEEE*

***Abstract*—Cognitive underlay amplify-and-forward (AF) two-way relay links require signal-to-interference-and-noise-ratio (SINR) balancing and maximizing strategies. And both secondary-to-primary and primary-to-secondary interference must be taken into consideration. To achieve these goals, we develop several joint distributed beamforming and power allocation algorithms. The development is based on the assumption of the availability of channel state information (CSI) of the relay-transceiver channels and the second-order-statistics (SOS) of all channels. For single-relay and multi-relay systems, a closed-form solution and an exhaustive-search optimal algorithm, respectively, are developed. This optimal algorithm, despite its high computational complexity, serves as a useful benchmark. Moreover, two low-complexity suboptimal algorithms are proposed, both of which compute sub-optimal power allocations and beamformers. A 10-dB SINR improvement by the optimal algorithm and similar gains by both proposed suboptimal algorithms are achievable.**

***Index Terms*—Amplify-and-forward relaying, cognitive radio, distributed beamforming, power allocation, second-order statistics of channel gains, SINR balancing, two-way relay, underlay.**

I. Introduction

DYNAMIC SPECTRUM ACCESS (DSA) addresses the dual problems of under-utilization of the licensed spectrum [1] and dramatically growing demand for wireless radio spectrum[2], [3]. Specifically, cognitive radio, which includes a hierarchical DSA model [4], has been studied widely because of its compatibility with the existing spectrum management policies[2]. Spectrum sharing cognitive radio networks allow cognitive radio users (secondary users) to share the spectrum bands of the licensed-band users (primary users). However, the secondary users must restrict their transmit power so that the interference caused to the primary users is kept below a predefined threshold (known as interference temperature limit I_{th}). Three common secondary access strategies [5] are

1) Interweave – a secondary user transmits only when no primary user transmits,
2) Overlay – secondary users facilitate primary user communications and in turn are allowed to transmit simultaneously provided the interference on primary receivers is below I_{th} [4],
3) Underlay – simultaneous primary and secondary transmissions are permitted provided the interference on primary receivers is below I_{th}.

In this paper, the underlay strategy is our focus. Specifically, we consider two secondary underlay users (or equivalently transceivers) requiring bidirectional data exchange. Unfortunately, the link performance of the two users (denoted by SU_1 and SU_2) degrades due to two reasons: (a) interference from primary nodes and (b) reduction of SU_1 and SU_2 transmit powers to satisfy I_{th}. To mitigate this link performance degradation, we use a low-complexity amplify-and-forward (AF) relay. However, we know that one-way half-duplex relays lose spectral efficiency. This loss is overcome by two-way relays operating over two time slots [6]. Consequently, we will use the two-way relay.

Moreover, multiple, spatially-separated relays allow their antenna gain adjustments (i.e., distributed beamforming) to exploit multi-user cooperative diversity [7]–[9], providing more robust communication links in fading and interference [10]. Thus, distributed beamforming improves outage probability and data rates and is implemented, subject to interference constraints, to maximize the signal-to-interference-and-noise-ratio (SINR), which also must be balanced between the two secondary terminals, giving higher power efficiency [11]. To achieve these goals, we optimally allocate the signal powers of SU_1 and SU_2 and adjust antenna gains (i.e., beamforming) to balance and maximize SINR. Note that in the resulting network (see Fig. 1), primary-to-secondary (P2S) and secondary-to-primary (S2P) interferences over two time slots must be taken into consideration.

For non-cognitive systems (i.e., no interference issues), several power allocation and beamforming algorithms for two-way relays have been studied recently [12]–[19]. For example, [12], [13] studied joint AF beamforming, antenna selection and optimal and sub-optimal power allocation schemes. In addition, the performance of zero-forcing beamforming was analyzed in [14]. In [15]–[19], the use of joint power allocation and beamforming was studied. The achievable rate region was general-

Manuscript received September 24, 2013; revised February 14, 2014 and July 11, 2014; accepted September 02, 2014. Date of publication September 17, 2014; date of current version October 24, 2014. The associate editor coordinating the review of this manuscript and approving it for publication was Prof. Zhengdao Wang.

Y. Cao is with the Department of Electrical and Computer Engineering, University of Alberta, Edmonton, AB T6G 2V4 Canada (e-mail: cao7@ualberta.ca; jessica.c0212@gmail.com).

C. Tellambura is with the Department of Electrical and Computer Engineering, University of Alberta, Edmonton, AB T6G 2V4 Canada (e-mail: chintha@ece.ualberta.ca).

Color versions of one or more of the figures in this paper are available online at http://ieeexplore.ieee.org.

Digital Object Identifier 10.1109/TSP.2014.2358953

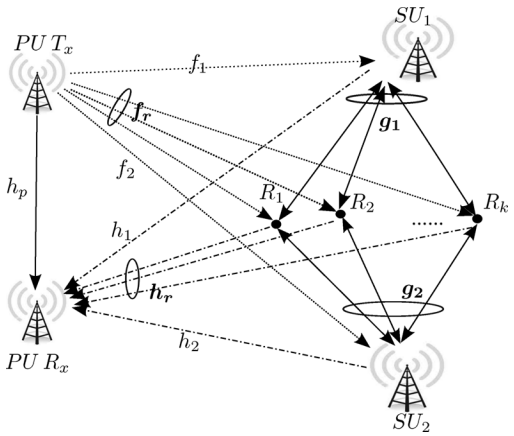

Fig. 1. Cognitive Two-Way Relay System.

ized in [15]. The power minimization problem was studied in [16] and [17], while the SNR balancing approaches, where the smaller signal-to-noise-ratio (SNR) of the two transceivers is maximized, were studied in [17]–[19] under total and individual power constraints. All these studies assumed the availability of perfect instantaneous channel state information (CSI).

For cognitive systems, almost all studies consider S2P interference only (i.e., only signal-to-noise-ratio (SNR) is considered). Moreover, the availability of perfect CSI is also assumed. For example, with AF relaying, beamforming and power allocation for overlay [20]–[24] and underlay [11], [25]–[29] cognitive relay systems have been developed. References [25] and [26] studied one-way multi-antenna relays. And [27] investigated one-way single-antenna relays. In [11], [28], [29], beamforming coefficients were derived for two-way relays.

However, the provision of full instantaneous CSI at all nodes is difficult in practical systems due to channel estimation and feedback overheads. So is it possible to reduce the overhead of full CSI? Partial CSI may be the answer and it involves: (1) the second-order-statistics (SOS) of all the channels at both SU_1 and SU_2; and (2) perfect instantaneous CSI of the channels from SU_i ($i = 1\,2$) to the relays available at SU_i. Clearly, the provision of partial CSI is less burdensome than that of full CSI in terms of channel estimation overheads. To the best of our knowledge, the use of partial CSI for joint distributed beamforming and power allocation for cognitive two-way relays considering both S2P and P2S interferences has not previously been studied. The main contributions of this paper thus include:

- The secondary SINR's are balanced and maximized taking into account the interference from the primary transmissions, subject to the secondary-to-primary interference constraints in both time slots.
- With partial CSI, the SINR balancing and maximizing requires adjusting the transmit powers, P_1 and P_2 of the two secondary transceivers respectively, and the relay beamforming coefficients. The feasible power allocations $(P_1,\ P_2)$ is a two-dimensional region. However, we show that the optimal $(P_1,\ P_2)$ lies on a trajectory crossing the feasible region.
- For a single relay, the closed-form optimal beamformer and power allocation are developed, where the optimal beamforming coefficient is limited to real values, rather than complex values. Therefore the phase distortion in the signal introduced by the complex channel gain is not explored, which leads to the limited system performance.
- For $K > 1$ relays, an exhaustive-search multi-relay optimal algorithm (MRO) is proposed. This algorithm uses combined bi-section search [30] and interior-point algorithm [30] to find the optimal beamformer. Despite its high complexity, this algorithm serves as a benchmark to evaluate sub-optimal algorithms.
- To reduce the computational complexity, we also propose two sub-optimal algorithms (simple-power-allocation (SPA) and two-phase search (TPS)), where power allocation and beamformers are computed suboptimally. While SPA searches exhaustively along the quantified power allocation points, the computations at each point are simpler than those in MRO. Unlike SPA, TPS directly finds a sub-optimal power allocation. In terms of the achievable SINRs, TPS differs only 0.15 dB from MRO, while SPA differs from MRO less than 0.8 dB and 1.5 dB in stabler channels and more fluctuating channels, respectively. On the other hand, compared to the exhaustive-search based MRO, both TPS and SPA can reduce over 90% running time (see Section IV-C for detailed analysis and discussion).
- Moreover, numerical results also show that our proposed joint distributed beamforming and power allocation improves SINR by 10 dB or more.

The remainder of this paper is organized as follows. Section II describes the system configuration and formulates the optimization problem. The optimal algorithms are developed in Section III for both single- and multi-relay systems, followed by two sub-optimal algorithms proposed in Section IV. Section V evaluates and compares the optimal and sub-optimal approaches. And the paper is concluded in Section VI.

Throughout this paper, bold lower-case italics and bold upper-case italics indicate vectors and matrices, respectively. $(\bullet)^*$, $(\bullet)^T$, $(\bullet)^{-1}$ and $(\bullet)^H$ represent complex matrix conjugation, transpose, inverse, and Hermitian transpose, respectively. In addition, $\lambda_{\max}(\boldsymbol{A},\ \boldsymbol{B})$ and $\lambda_{\min}(\boldsymbol{A},\ \boldsymbol{B})$ stand for the maximum and minimum generalized eigenvalues of the matrix pair $(\boldsymbol{A},\ \boldsymbol{B})$. $\boldsymbol{A} \circ \boldsymbol{B}$ is the Hadamard product of the two matrices. Furthermore, $diag(\boldsymbol{\alpha})$ denotes a diagonal matrix with the diagonal vector $\boldsymbol{\alpha}$. $\| \bullet \|$ is the Euclidean norm, and $\mathbb{E}\{\bullet\}$ stands for the statistical expectation.

II. System Model and Problem Formulation

A. System Setup

This paper employs the following assumptions. The system (Fig. 1) is a secondary network that coexists with a primary network via the underlay approach. In the primary network, the transmitter $PU\ T_x$ communicates with the receiver $PU\ R_x$ through channel h_p. No direct link exists between the two secondary transceivers SU_1 and SU_2, and they communicate via half-duplex relay nodes R_i ($i = 1, 2, \ldots, K$). Perfect timing synchronization among the relays and the two

secondary transceivers is assumed. Stationary, mutually-independent, flat-fading channels with additive white Gaussian noise (AWGN) are assumed.

AF relays use two consecutive time slots for one-round information exchange between SU_1 and SU_2. In the first time slot, $PU\,T_x$ transmits $x^{(1)}$ to $PU\,R_x$ with power P_p. In the meantime, SU_j transmits s_j to the relays by using power P_j ($j = 1, 2$) through the reciprocal channels $\boldsymbol{g}_j = [g_{j_1}, g_{j_2}, \ldots, g_{j_K}]^T$, where g_{j_i} ($j = 1, 2$; $i = 1, 2, \ldots, K$) is the complex channel gain between SU_j and R_i. Consequently, the ith relay receives signal r_i as

$$r_i = \sqrt{P_1} g_{1i} s_1 + \sqrt{P_2} g_{2i} s_2 + \sqrt{P_p} f_{r_i} x^{(1)} + n_{r_i}, \quad (1)$$

where f_{r_i} denotes the interference channel gain from $PU\,T_x$ to R_i, and n_{r_i} is the zero-mean AWGN of variance σ_r^2. Due to the transmissions of SU_1 and SU_2, the interference signal $x_{int}^{(1)}$ received at PUR_x is given as

$$x_{int}^{(1)} = \sqrt{P_1} h_1 s_1 + \sqrt{P_2} h_2 s_2, \quad (2)$$

where h_j ($j = 1, 2$) indicates the interference channel gain from SU_j to $PU\,R_x$.

In the second time slot, $PU\,T_x$ transmits $x^{(2)}$ still with power P_p, while each relay multiplies its received signal r_i with a complex beamforming coefficient ω_i, and broadcasts the resulting signal to SU_j ($j = 1, 2$). The interference signal $x_{int}^{(2)}$ at PUR_x caused by the transmissions of all the relays is given as

$$x_{int}^{(2)} = \sqrt{P_1}\boldsymbol{\omega}\boldsymbol{H}_r\boldsymbol{g}_1 s_1 + \sqrt{P_2}\boldsymbol{\omega}\boldsymbol{H}_r\boldsymbol{g}_2 s_2 + \sqrt{P_p}\boldsymbol{\omega}\boldsymbol{H}_r\boldsymbol{f}_r x^{(1)} + \boldsymbol{\omega}\boldsymbol{H}_r\boldsymbol{n}_r, \quad (3)$$

where $\boldsymbol{H}_r = diag\{\boldsymbol{h}_r\}$, and $\boldsymbol{h}_r$ represents the interference channel gains from relays to $PU\,R_x$.

The signal y_j received at SU_j is given as

$$y_j = \underbrace{\sqrt{P_j}\boldsymbol{\omega}\boldsymbol{G}_j\boldsymbol{g}_j s_j}_{\text{self-interference}} + \underbrace{\sqrt{P_{\bar{j}}}\boldsymbol{\omega}\boldsymbol{G}_j\boldsymbol{g}_{\bar{j}} s_{\bar{j}}}_{\text{signal}} + \underbrace{\sqrt{P_p}\boldsymbol{\omega}\boldsymbol{G}_j\boldsymbol{f}_r x^{(1)} + \sqrt{P_p} f_j x^{(2)}}_{\text{interference}} + \underbrace{\boldsymbol{\omega}\boldsymbol{G}_j\boldsymbol{n}_r + n_j}_{\text{noise}}, \quad (4)$$

where $\boldsymbol{f}_r = [f_{r_1}, f_{r_2}, \ldots, f_{r_K}]^T$, $\boldsymbol{\omega} = [\omega_1, \omega_2, \ldots, \omega_K]$, $\boldsymbol{n}_r = [n_{r_1}, n_{r_2}, \ldots, n_{r_K}]^T$, $\boldsymbol{G}_j = diag\{\boldsymbol{g}_j\}$, f_j denotes the interference channel gain from $PU\,T_x$ to SU_j, n_j ($j = 1, 2$) is the AWGN of zero mean and variance σ_j^2, and $\bar{j} = 1$ if $j = 2$, and vise versa.

We assume that SU_j ($j = 1, 2$) obtains the instantaneous CSI of $\boldsymbol{g}_j$ by pilot-assisted two-way relay channel estimation methods [31]. But estimation of $\boldsymbol{g}_i$ ($i \neq j$) by SU_j is challenging because of the time-varying nature of wireless channels [32]. Moreover, exchange of CSI among nodes requires significant overhead for multiple nodes. These challenges of providing instant CSI can be mitigated by the use of channel statistics, which will stay constant for relatively long durations and hence can reduce the overhead. Consequently, we assume the SOS of all the channels, $\mathbb{E}\{\boldsymbol{g}_j\boldsymbol{g}_j^H\}$ ($j = 1, 2$), are available at both secondary transceivers. In contrast, because the existence of the secondary users is transparent to the primary users, they do not know the primary-secondary channels. Moreover, without loss of generality, we assume unit symbol power, $\mathbb{E}\{\|x\|^2\} = \mathbb{E}\{\|s_1\|^2\} = \mathbb{E}\{\|s_2\|^2\} = 1$. To reduce the overhead, the secondary transceivers compute power allocation and beamforming coefficients, and use an error-free feedback channel to transmit this information to the relays.

By knowing $\boldsymbol{\omega}$, $\boldsymbol{g}_j$ and s_j, SU_j ($j = 1, 2$) can eliminate its self-interference perfectly. Consequently, the self-interference-free signal $\tilde{y_j}$ ($j = 1, 2$) is given as

$$\tilde{y_j} = \underbrace{\sqrt{P_{\bar{j}}}\boldsymbol{\omega}\boldsymbol{G}_j\boldsymbol{g}_{\bar{j}} s_{\bar{j}}}_{\text{signal}} + \underbrace{\sqrt{P_p}\boldsymbol{\omega}\boldsymbol{G}_j\boldsymbol{f}_r x^{(1)} + \sqrt{P_p} f_j x^{(2)}}_{\text{interference}} + \underbrace{\boldsymbol{\omega}\boldsymbol{G}_j\boldsymbol{n}_r + n_j}_{\text{noise}}. \quad (5)$$

B. Problem Formulation

The average SINR at SU_j ($j = 1, 2$) is considered, which is given as

$$\begin{aligned}
\text{SINR}_j &= \frac{P_{\bar{j}}\boldsymbol{\omega}\boldsymbol{A}\boldsymbol{\omega}^H}{\boldsymbol{\omega}(\boldsymbol{B}_j + \boldsymbol{B}_{N_j})\boldsymbol{\omega}^H + \hat{\sigma_j^2}},\\
\text{where } \boldsymbol{A} &\triangleq \mathbb{E}\{\boldsymbol{G}_1\boldsymbol{g}_2\boldsymbol{g}_2^H\boldsymbol{G}_1^H\}\\
&= \mathbb{E}\{\boldsymbol{g}_1\boldsymbol{g}_1^H\} \circ \mathbb{E}\{\boldsymbol{g}_2\boldsymbol{g}_2^H\},\\
\boldsymbol{B}_j &\triangleq P_p\mathbb{E}\{\boldsymbol{G}_j\boldsymbol{f}_r\boldsymbol{f}_r^H\boldsymbol{G}_j^H\}\\
&= P_p\mathbb{E}\{\boldsymbol{g}_j\boldsymbol{g}_j^H\} \circ \mathbb{E}\{\boldsymbol{f}_r\boldsymbol{f}_r^H\},\\
\sigma_{f_j}^2 &= P_p\mathbb{E}\{f_j f_j^*\},\\
\boldsymbol{B}_{N_j} &\triangleq \sigma_r^2\mathbb{E}\{\boldsymbol{G}_j\boldsymbol{G}_j^H\} \triangleq \sigma_r^2 diag\{\mathbb{E}\{g_{ji}g_{ji}^*\}\},\\
\hat{\sigma_j^2} &\triangleq \sigma_{f_j}^2 + \sigma_j^2. \quad (6)
\end{aligned}$$

On the other hand, the average interference powers at PUR_x in time slot one ($P_I^{(1)}$) and two ($P_I^{(2)}$) are given as

$$\begin{aligned}
P_I^{(1)} &= a_1 P_1 + a_2 P_2, \quad (7a)\\
P_I^{(2)} &= \boldsymbol{\omega}(P_1\boldsymbol{C}_1 + P_2\boldsymbol{C}_2 + \boldsymbol{C}_3)\boldsymbol{\omega}^H,\\
\text{where } a_1 &\triangleq \mathbb{E}\{h_1 h_1^*\},\ a_2 \triangleq \mathbb{E}\{h_2 h_2^*\},\\
\boldsymbol{C}_1 &\triangleq \mathbb{E}\{\boldsymbol{H}_r\boldsymbol{g}_1\boldsymbol{g}_1^H\boldsymbol{H}_r^H\} = \mathbb{E}\{\boldsymbol{g}_1\boldsymbol{g}_1^H\} \circ \mathbb{E}\{\boldsymbol{h}_r\boldsymbol{h}_r^H\},\\
\boldsymbol{C}_2 &\triangleq \mathbb{E}\{\boldsymbol{H}_r\boldsymbol{g}_2\boldsymbol{g}_2^H\boldsymbol{H}_r^H\} = \mathbb{E}\{\boldsymbol{g}_2\boldsymbol{g}_2^H\} \circ \mathbb{E}\{\boldsymbol{h}_r\boldsymbol{h}_r^H\},\\
\boldsymbol{C}_3 &\triangleq P_p\mathbb{E}\{\boldsymbol{H}_r\boldsymbol{f}_r\boldsymbol{f}_r^H\boldsymbol{H}_r^H\} + \sigma_r^2\mathbb{E}\{\boldsymbol{H}_r\boldsymbol{H}_r^H\}. \quad (7b)
\end{aligned}$$

Our goal is to jointly design the beamforming vector $\boldsymbol{\omega}$ and power allocation (P_1, P_2), such that the minimum of SINR_1 and SINR_2 is maximized while both $P_I^{(1)}$ and $P_I^{(2)}$ are under a

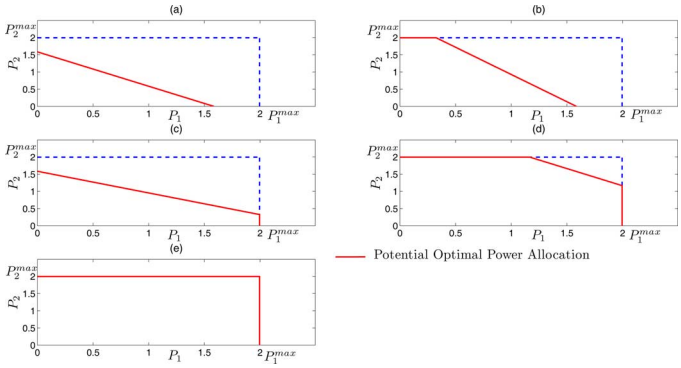

Fig. 2. Five Cases of POPA Line. (a) Case I: $a_1P_1 + a_2P_2 = I_{th}$ is inside the rectangular from $(0, 0)$ to $(P_1^{\max}, P_2^{\max})$. (b) Case II: $a_1P_1 + a_2P_2 = I_{th}$ is outside the rectangular when $P_2 > P_2^{\max}$. (c) Case III: $a_1P_1 + a_2P_2 = I_{th}$ is outside the rectangular when $P_1 > P_1^{\max}$. (d) Case IV: $a_1P_1 + a_2P_2 = I_{th}$ is outside the rectangular when $P_j > P_j^{\max}$, $j = 1, 2$. (e) Case V: $a_1P_1 + a_2P_2 = I_{th}$ is outside the rectangular.

predefined threshold I_{th}. Additionally, P_1 and P_2 should not exceed their maximum available levels, namely $P_1^{\max}$ and $P_2^{\max}$, respectively. Accordingly, the optimization problem is formed as

$$\text{(P-1)} \quad \max_{P_1,\,P_2,\,\boldsymbol{\omega}} \quad \min\{\text{SINR}_1, \text{SINR}_2\}$$
$$\text{s.t.} \quad \boldsymbol{\omega}(P_1\boldsymbol{C}_1 + P_2\boldsymbol{C}_2 + \boldsymbol{C}_3)\boldsymbol{\omega}^H \le I_{th}, \quad (8a)$$
$$a_1P_1 + a_2P_2 \le I_{th}, \quad (8b)$$
$$P_1 \le P_1^{\max},\ P_2 \le P_2^{\max}, \quad (8c)$$
$$\text{where} \quad \text{SINR}_1 = \frac{P_2\boldsymbol{\omega}\boldsymbol{A}\boldsymbol{\omega}^H}{\boldsymbol{\omega}(\boldsymbol{B}_1 + \boldsymbol{B}_{N_1})\boldsymbol{\omega}^H + \hat{\sigma_1^2}},$$
$$\text{SINR}_2 = \frac{P_1\boldsymbol{\omega}\boldsymbol{A}\boldsymbol{\omega}^H}{\boldsymbol{\omega}(\boldsymbol{B}_2 + \boldsymbol{B}_{N_2})\boldsymbol{\omega}^H + \hat{\sigma_2^2}}.$$

Lemma 1: (P-1) is an SINR balancing problem and there is one optimal solution $(P_1, P_2, \boldsymbol{\omega})$ *such that (P-1) achieves its optimal value with* $\text{SINR}_1 = \text{SINR}_2$.

Proof: See Appendix A. ■

Lemma 2: Let $(P_1^{opt}, P_2^{opt}, \boldsymbol{\omega}^{opt})$ *be one optimal solution to (P-1). Then at least one of the three inequality constraints in (8b) and (8c) are satisfied with equality.*

Proof: See Appendix B. ■

According to Lemma 2, the optimal power allocation (P_1, P_2) must lie on the lines formed by (8b) and (8c). In the remaining of this paper, we refer to these lines as the Potential Optimal Power Allocation (POPA) line. Fig. 2 shows the five possible cases of the POPA line: (1) in the first case, the POPA line is totally determined by the interference constraint (8b) in time slot one, as shown in Fig. 2(a); (2) in the second case, it is determined by $P_2 < P_2^{\max}$ and (8b), as shown in Fig. 2(b); (3) in the third case, it is determined by $P_1 < P_1^{\max}$ and (8b), as shown in Fig. 2(c), (4) in the fourth case, it is determined by both (8b) and (8c), as shown in Fig. 2(d); (5) in the fifth case, the POPA line is determined by only (8c), as shown in Fig. 2(e).

Lemma 3: Let $(P_1^{opt}, P_2^{opt}, \boldsymbol{\omega}^{opt})$ *be one optimal solution to (P-1). Then the inequality constraint (8a) is satisfied with equality.*

Proof: See Appendix C. ■

III. Optimal Beamforming and Power Allocation

In this section, a closed-form solution to (P-1) is developed first when a single relay serves the secondary network. For multiple relays, (P-1) is reformulated to derive optimal exhaustive search algorithm.

A. Single-Relay System

In a single-relay system, all vectors and matrices become scales and are presented in lower-case letters throughout this section. Then the optimization problem (P-1) becomes

$$\text{(P-2)} \quad \max_{P_1,\,P_2,\,\omega} \min\left\{\frac{P_2\|g_1\|^2\|g_2\|^2\|\omega\|^2}{\Delta\|g_1\|^2\|\omega\|^2 + \hat{\sigma_1^2}}, \frac{P_1\|g_1\|^2\|g_2\|^2\|\omega\|^2}{\Delta\|g_2\|^2\|\omega\|^2 + \hat{\sigma_2^2}}\right\}$$
$$\text{s.t.} \quad \|h_r\|^2(P_1\|g_1\|^2 + P_2\|g_2\|^2 + \Delta)\|\omega\|^2 \le I_{th}, \quad (9a)$$
$$a_1P_1 + a_2P_2 \le I_{th}, \quad (9b)$$
$$P_1 \le P_1^{\max},\ P_2 \le P_2^{\max}, \quad (9c)$$
$$\|g_j\|^2 \triangleq \mathbb{E}\{\|g_j\|^2\}, \|f_j\|^2 \triangleq \mathbb{E}\{\|f_j\|^2\},\ j = 1, 2,$$
$$\|h_r\|^2 \triangleq \mathbb{E}\{\|h_r\|^2\}, \|f_r\|^2 \triangleq \mathbb{E}\{\|f_r\|^2\}, \Delta \triangleq P_p\|f_r\|^2 + \sigma_r^2.$$

Algorithm SRO: Closed-Form Solution for Single-Relay Systems

Input : Δ, $\|h_r\|^2$, $\|g_1\|^2$, $\|g_2\|^2$, $\hat{\sigma_1^2}$, $\hat{\sigma_2^2}$, a_1, a_2, $P_1^{\max}$, $P_2^{\max}$, I_{th}

Output: P_1, P_2, ω

if $\|g_1\|^2\hat{\sigma_2^2} = \|g_2\|^2\hat{\sigma_1^2}$ **then**

  $P_1 = \frac{\hat{\sigma_2^2}}{\hat{\sigma_1^2}}P_2$,

  $P_2 = \min\left(\frac{\hat{\sigma_1^2}}{\hat{\sigma_2^2}}P_1^{\max}, P_2^{\max}, \frac{\hat{\sigma_1^2}I_{th}}{a_1\hat{\sigma_2^2} + a_2\hat{\sigma_1^2}}\right)$,

  $\omega = \sqrt{\frac{I_{th}}{\|h_r\|^2(P_1\|g_1\|^2 + P_2\|g_2\|^2 + \Delta)}}$;

else

  Compute $(P_1^{(1)}, P_2^{(1)})$, $(P_1^{(2)}, P_2^{(2)})$ and $(P_1^{(3)}, P_2^{(3)})$ via equations **(10a)–(10c)** at the bottom of the next page;

  Choose the point on the POPA line from $(P_1^{(1)}, P_2^{(1)})$, $(P_1^{(2)}, P_2^{(2)})$ and $(P_1^{(3)}, P_2^{(3)})$ as the optimal power allocation;

  $\omega = \sqrt{\frac{P_2\hat{\sigma_2^2} - P_1\hat{\sigma_1^2}}{(P_1\|g_1\|^2 - P_2\|g_2\|^2)\Delta}}$;

end

return P_1, P_2, ω.

A closed-form solution to (P-2) can be found by using the SRO Algorithm. According to (P-2), the phase of ω has no impact on the solution. Therefore, we assume that ω takes only a positive real value. Furthermore, applying Lemma 1 and Lemma 3, the original three dimensional optimization problem turns into a two dimensional optimization problem as

$$\begin{aligned}(\text{P-3}) \quad \max_{P_1,\,P_2} \quad & \frac{\|g_1\|^2\|g_2\|^2(P_2\hat{\sigma_2^2}-P_1\hat{\sigma_1^2})}{\Delta(\|g_1\|^2\hat{\sigma_2^2}-\|g_2\|^2\hat{\sigma_1^2})}\\ \text{s.t.} \quad & \Phi(P_1,\,P_2)=0, && \text{(11a)}\\ & a_1P_1+a_2P_2\le I_{th}, && \text{(11b)}\\ & P_1\le P_1^{\max}, P_2\le P_2^{\max}, && \text{(11c)}\\ & \|\omega\|^2=\frac{P_2\hat{\sigma_2^2}-P_1\hat{\sigma_1^2}}{(P_1\|g_1\|^2-P_2\|g_2\|^2)\Delta}>0. && \text{(11d)}\end{aligned}$$

$$\begin{aligned}\text{where } \Phi(P_1,P_2) \triangleq\ & \|h_r\|^2\|g_2\|^2\hat{\sigma_2^2}P_2^2-\|h_r\|^2\|g_1\|^2\hat{\sigma_1^2}P_1^2\\ & +(\|h_r\|^2\|g_1\|^2\hat{\sigma_2^2}-\|h_r\|^2\|g_2\|^2\hat{\sigma_1^2})P_1P_2\\ & +(\Delta\|h_r\|^2\hat{\sigma_2^2}+\Delta I_{th}\|g_2\|^2)P_2\\ & -(\Delta\|h_r\|^2\hat{\sigma_1^2}+\Delta I_{th}\|g_1\|^2)P_1. \qquad \text{(12)}\end{aligned}$$

There are three possible cases for (P-3):

1) Case 1: $\|g_1\|^2\hat{\sigma_2^2}>\|g_2\|^2\hat{\sigma_1^2}$: In order to keep both SINRs and $\|\omega\|^2$ positive, $(P_1,\,P_2)$ must satisfy

$$\frac{\hat{\sigma_1^2}}{\hat{\sigma_2^2}}<\frac{P_2}{P_1}<\frac{\|g_1\|^2}{\|g_2\|^2} \qquad (13)$$

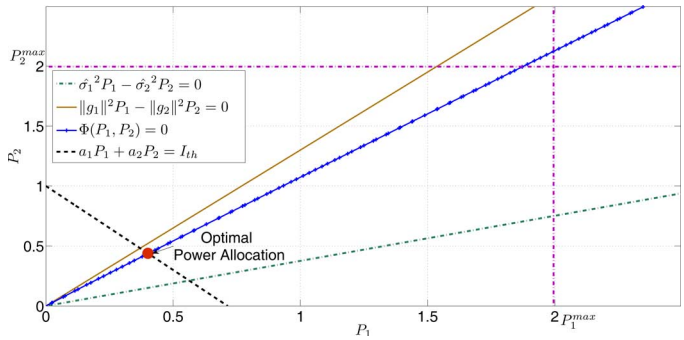

Fig. 3. Single-Relay Cognitive System, Case 1: $\|g_1\|^2\hat{\sigma_2^2}>\|g_2\|^2\hat{\sigma_1^2}$.

In addition, $\Phi(P_1,\,P_2)=0$ is a hyperbolic curve, which always lies between the lines $P_2=\frac{\hat{\sigma_1^2}}{\hat{\sigma_2^2}}P_1$ and $P_2=\frac{\|g_1\|^2}{\|g_2\|^2}P_1$ in the first phase, as shown in Fig. 3. Accordingly, (P-3) can be reformulated as

$$\begin{aligned}(\text{P-4}) \quad \max_{P_1,\,P_2} \quad & \frac{\|g_1\|^2\|g_2\|^2(P_2\hat{\sigma_2^2}-P_1\hat{\sigma_1^2})}{\Delta(\|g_1\|^2\hat{\sigma_2^2}-\|g_2\|^2\hat{\sigma_1^2})}\\ \text{s.t.} \quad & \Phi(P_1,\,P_2)=0,\\ & a_1P_1+a_2P_2\le I_{th},\\ & P_1\le P_1^{\max},\ P_2\le P_2^{\max}.\end{aligned}$$

Moreover, Lemma 2 implies that the optimal power allocation should be the crosspoint of $\Phi(P_1,\,P_2)=0$ and the POPA line, which must be one of (10a)–(10c), shown at the bottom of the page. An example of this case is shown in Fig. 3.

$$P_1^{(1)}=\frac{-\xi_1-\sqrt{\xi_1^2-4\zeta_1\varrho_1}}{2\zeta_1},P_2^{(1)}=P_2^{\max}, \qquad (10a)$$

$$P_1^{(2)}=P_1^{\max},P_2^{(2)}=\frac{-\xi_2+\sqrt{\xi_2^2-4\zeta_2\varrho_2}}{2\zeta_2}, \qquad (10b)$$

$$P_1^{(3)}=\frac{-\xi_3-\sqrt{\xi_3^2-4\zeta_3\varrho_3}}{2\zeta_3},P_2^{(3)}=\frac{I_{th}}{a_1}-\frac{a_1}{a_2}P_1^{(3)}, \qquad (10c)$$

$$\begin{aligned}\text{where } \xi_1=&\|h_r\|^2(\|g_1\|^2\hat{\sigma_2^2}-\|g_2\|^2\hat{\sigma_1^2})P_2^{\max}-\Delta(\|h_r\|^2\hat{\sigma_1^2}+I_{th}\|g_1\|^2),\\ \zeta_1=&-\|h_r\|^2\|g_1\|^2\hat{\sigma_1^2},\\ \varrho_1=&\|h_r\|^2\|g_2\|^2\hat{\sigma_2^2}P_2^{\max^2}+(\|h_r\|^2\hat{\sigma_2^2}+I_{th}\|g_2\|^2)\Delta P_2^{\max},\\ \xi_2=&\|h_r\|^2(\|g_1\|^2\hat{\sigma_2^2}-\|g_2\|^2\hat{\sigma_1^2})P_1^{\max}+\Delta(\|h_r\|^2\hat{\sigma_2^2}+I_{th}\|g_2\|^2),\\ \zeta_2=&\|h_r\|^2\|g_2\|^2\hat{\sigma_2^2},\\ \varrho_2=&-\|h_r\|^2\|g_1\|^2\hat{\sigma_1^2}P_1^{\max^2}-(\|h_r\|^2\hat{\sigma_1^2}+I_{th}\|g_1\|^2)\Delta P_1^{\max},\\ \xi_3=&-\frac{2I_{th}a_1\|h_r\|^2\|g_2\|^2\hat{\sigma_2^2}}{a_2^2}-\frac{\|h_r\|^2\hat{\sigma_2^2}+I_{th}\|g_2\|^2}{a_2}\Delta a_1\\ &-(\|h_r\|^2\hat{\sigma_1^2}+I_{th}\|g_1\|^2)\Delta+\frac{(\|g_1\|^2\hat{\sigma_2^2}-\|g_2\|^2\hat{\sigma_1^2})I_{th}\|h_r\|^2}{a_2},\\ \zeta_3=&\frac{\|h_r\|^2\|g_2\|^2\hat{\sigma_2^2}a_1^2}{a_2^2}-\frac{(\|g_1\|^2\hat{\sigma_2^2}-\|g_2\|^2\hat{\sigma_1^2})\|h_r\|^2a_1}{a_2}-\|h_r\|^2\|g_1\|^2\hat{\sigma_1^2},\\ \varrho_3=&\frac{\|h_r\|^2\|g_2\|^2\hat{\sigma_2^2}I_{th}^2}{a_2^2}+\frac{(\|h_r\|^2\hat{\sigma_2^2}+I_{th}\|g_2\|^2)I_{th}\Delta}{a_2}.\end{aligned}$$

2) Case 2: $\|g_1\|^2\hat{\sigma_2^2} < \|g_2\|^2\hat{\sigma_1^2}$*:* The proof of *CASE 2* is similar to that of *CASE 1*, which leads to the same closed-form solution.

Algorithm MBSS: Modified Bi-Section Search

Input : P_1, P_2, $\boldsymbol{A}$, $\boldsymbol{B}_1$, $\boldsymbol{B}_{N_1}$, $\boldsymbol{B}_2$, $\boldsymbol{B}_{N_2}$, $\hat{\sigma_1^2}$, $\hat{\sigma_2^2}$, $\boldsymbol{C}_1$, $\boldsymbol{C}_2$, $\boldsymbol{C}_3$, I_{th}

Output: t, $\boldsymbol{\omega}$

Internal Variables : t_u, t_l, t_m, $\tilde{\boldsymbol{\omega}}_m$

Compute $\boldsymbol{C} = P_1\boldsymbol{C}_1 + P_2\boldsymbol{C}_2 + \boldsymbol{C}_3$;

Compute $\boldsymbol{C}^{1/2}$ and $\boldsymbol{C}^{-1/2}$ such that $\boldsymbol{C}^{1/2}\boldsymbol{C}^{1/2} = \boldsymbol{C}$;

Compute $\hat{\boldsymbol{A}}_1$, $\hat{\boldsymbol{A}}_2$, $\hat{\boldsymbol{B}}_1$, $\hat{\boldsymbol{B}}_2$ by using **(16)**;

Compute $(t_i, \tilde{\boldsymbol{\omega}}_i)$, $i = 1, 2$ such that $t_i = \lambda_{\max}(\hat{\boldsymbol{A}}_i, \hat{\boldsymbol{B}}_i)$, where $\tilde{\boldsymbol{\omega}}_i$ is the corresponding normalized eigenvector to $\lambda_{\max}(\hat{\boldsymbol{A}}_i, \hat{\boldsymbol{B}}_i)$;

if $t_1 < t_2$ **then**

$$t_u = t_1, \tilde{\boldsymbol{\omega}}_m = \tilde{\boldsymbol{\omega}}_1, t_l = \frac{\tilde{\boldsymbol{\omega}}_m\hat{\boldsymbol{A}}_2\tilde{\boldsymbol{\omega}}_m^H}{\tilde{\boldsymbol{\omega}}_m\hat{\boldsymbol{B}}_2\tilde{\boldsymbol{\omega}}_m^H};$$

else if $t_1 > t_2$ **then**

$$t_u = t_2, \tilde{\boldsymbol{\omega}}_m = \tilde{\boldsymbol{\omega}}_2, t_l = \frac{\tilde{\boldsymbol{\omega}}_m\hat{\boldsymbol{A}}_1\tilde{\boldsymbol{\omega}}_m^H}{\tilde{\boldsymbol{\omega}}_m\hat{\boldsymbol{B}}_1\tilde{\boldsymbol{\omega}}_m^H};$$

else

$$t_u = t_1, t_1' = \frac{\tilde{\boldsymbol{\omega}}_2\hat{\boldsymbol{A}}_1\tilde{\boldsymbol{\omega}}_2^H}{\tilde{\boldsymbol{\omega}}_2\hat{\boldsymbol{B}}_1\tilde{\boldsymbol{\omega}}_2^H}, t_2' = \frac{\tilde{\boldsymbol{\omega}}_1\hat{\boldsymbol{A}}_2\tilde{\boldsymbol{\omega}}_1^H}{\tilde{\boldsymbol{\omega}}_1\hat{\boldsymbol{B}}_2\tilde{\boldsymbol{\omega}}_1^H};$$

  if $t_1' \geq t_2'$ **then** $t_l = t_1', \tilde{\boldsymbol{\omega}}_m = \tilde{\boldsymbol{\omega}}_2$;

  else $t_l = t_2', \tilde{\boldsymbol{\omega}}_m = \tilde{\boldsymbol{\omega}}_1$;

  end

end

if $t_u \leq t_l$ **then** $t_m = t_u$;

else

  while $\|t_u - t_l\| > \eta$ **do**

    $t_m = \frac{t_u + t_l}{2}, \tilde{\boldsymbol{\omega}}_m = \boldsymbol{0}$;

    if *(P-8) with* $t = t_m$ *is feasible* **then** $t_l = t_m, \tilde{\boldsymbol{\omega}}_m =$ any solution of (P-8);

    else $t_u = t_m$;

    end;

  end

end

if $t_m \leq 0$ **then** $t = 0, \boldsymbol{\omega} = \boldsymbol{0}$;

else $t = t_m, \boldsymbol{\omega} = \sqrt{I_{th}}\tilde{\boldsymbol{\omega}}_m\boldsymbol{C}^{-1/2}$;

end

return t, $\boldsymbol{\omega}$.

3) Case 3: $\|g_1\|^2\hat{\sigma_2^2} = \|g_2\|^2\hat{\sigma_1^2}$*:* Although the probability that this case occurs is nearly zero, when it does happen we have the following approach to find out the optimal solution.

The SINR balancing property indicates that (P_1, P_2, ω) must fulfill both $P_1\hat{\sigma_1^2} = P_2\hat{\sigma_2^2}$ and $\|\omega\|^2 = I_{th}/[\|h_r\|^2(P_1\|g_1\|^2 + P_2\|g_2\|^2 + \Delta)]$. Then (P-4) is equivalent to

$$\text{(P-5)} \max_{P_2} \frac{P_2\|g_1\|^2\|g_2\|^2 I_{th}}{2\|h_r\|^2\|g_1\|^2\hat{\sigma_2^2}\hat{\sigma_1^2}P_2 + \hat{\sigma_1^2}\|g_1\|^2\Delta I_{th} + \|h_r\|^2\hat{\sigma_1^2}\Delta}$$
$$\text{s.t.} \quad P_2 \leq \frac{I_{th}\hat{\sigma_1^2}}{a_1\hat{\sigma_2^2} + a_2\hat{\sigma_1^2}},\ P_2 \leq \frac{\hat{\sigma_1^2}}{\hat{\sigma_2^2}}P_1^{\max},\ P_2 \leq P_2^{\max}.$$

It is obvious that (P-5) achieves its optimal value when

$$P_2 = \min\left(\frac{\hat{\sigma_1^2}}{\hat{\sigma_2^2}}P_1^{\max},\ P_2^{\max}, \frac{\hat{\sigma_1^2}I_{th}}{a_1\hat{\sigma_2^2} + a_2\hat{\sigma_1^2}}\right). \tag{14}$$

The analysis above is concluded as step 2 in the SRO algorithm.

B. Multi-Relay System

When multiple relays are present in the secondary network to assist the communication, a slack variable t can be introduced to (P-1), which results in

$$\begin{aligned}\text{(P-6)} \quad \max_{P_1, P_2, \boldsymbol{\omega}, t} \quad & t \\ \text{s.t.} \quad & \frac{P_2\boldsymbol{\omega}\boldsymbol{A}\boldsymbol{\omega}^H}{\boldsymbol{\omega}(\boldsymbol{B}_1 + \boldsymbol{B}_{N_1})\boldsymbol{\omega}^H + \hat{\sigma_1^2}} \geq t, \\ & \frac{P_1\boldsymbol{\omega}\boldsymbol{A}\boldsymbol{\omega}^H}{\boldsymbol{\omega}(\boldsymbol{B}_2 + \boldsymbol{B}_{N_2})\boldsymbol{\omega}^H + \hat{\sigma_2^2}} \geq t, \\ & \boldsymbol{\omega}(P_1\boldsymbol{C}_1 + P_2\boldsymbol{C}_2 + \boldsymbol{C}_3)\boldsymbol{\omega}^H = I_{th}, \\ & a_1P_1 + a_2P_2 \leq I_{th}, \\ & P_1 \leq P_1^{\max},\ P_2 \leq P_2^{\max}.\end{aligned}$$

This problem is a non-convex optimization problem. However, if we fix the transmit power (P_1, P_2), which satisfies $a_1P_1 + a_2P_2 \leq I_{th}$, $P_1 \leq P_1^{\max}$, $P_2 \leq P_2^{\max}$, the corresponding optimal beamformer $\boldsymbol{\omega}$ can be found as follows. Define the Hermitian and positive definite matrix $\boldsymbol{C} \triangleq P_1\boldsymbol{C}_1 + P_2\boldsymbol{C}_2 + \boldsymbol{C}_3$. Next, decompose $\boldsymbol{\omega}$ as, $\boldsymbol{\omega} \triangleq \sqrt{p}\tilde{\boldsymbol{\omega}}\boldsymbol{C}^{-1/2}$, where $\|\tilde{\boldsymbol{\omega}}\|^2 = 1$, $p \geq 0$, and $\boldsymbol{C}^{-1/2}$ is the inverse of $\boldsymbol{C}^{1/2}$. Clearly, p should take value of I_{th} to satisfy $\boldsymbol{\omega}(P_1\boldsymbol{C}_1 + P_2\boldsymbol{C}_2 + \boldsymbol{C}_3)\boldsymbol{\omega}^H = I_{th}$. Then (P-6) is simplified as

$$\begin{aligned}\text{(P-7)} \quad \max_{\tilde{\boldsymbol{\omega}}, t} \quad & t \\ \text{s.t.} \quad & \frac{\tilde{\boldsymbol{\omega}}\hat{\boldsymbol{A}}_1\tilde{\boldsymbol{\omega}}^H}{\tilde{\boldsymbol{\omega}}\hat{\boldsymbol{B}}_1\tilde{\boldsymbol{\omega}}^H} \geq t,\ \frac{\tilde{\boldsymbol{\omega}}\hat{\boldsymbol{A}}_2\tilde{\boldsymbol{\omega}}^H}{\tilde{\boldsymbol{\omega}}\hat{\boldsymbol{B}}_2\tilde{\boldsymbol{\omega}}^H} \geq t, \\ & \|\tilde{\boldsymbol{\omega}}\|^2 = 1,\ t > 0.\end{aligned} \tag{15}$$

where

$$\begin{cases}\hat{\boldsymbol{A}}_1 = P_2I_{th}\boldsymbol{C}^{-1/2}\boldsymbol{A}\boldsymbol{C}^{-1/2}, \\ \hat{\boldsymbol{A}}_2 = P_1I_{th}\boldsymbol{C}^{-1/2}\boldsymbol{A}\boldsymbol{C}^{-1/2}, \\ \hat{\boldsymbol{B}}_1 = I_{th}\boldsymbol{C}^{-1/2}(\boldsymbol{B}_1 + \boldsymbol{B}_{N_1})\boldsymbol{C}^{-1/2} + \hat{\sigma_1^2}I, \\ \hat{\boldsymbol{B}}_2 = I_{th}\boldsymbol{C}^{-1/2}(\boldsymbol{B}_2 + \boldsymbol{B}_{N_2})\boldsymbol{C}^{-1/2} + \hat{\sigma_2^2}I.\end{cases} \tag{16}$$

Problem (P-7) can be solved by using the bi-section search [30], and with each fixed $t = t_m$, the problem is reduced to a feasibility problem [30] as

$$\text{(P-8)} \quad \text{Find} \quad \tilde{\boldsymbol{\omega}} \\ \text{s.t.} \quad \frac{\tilde{\boldsymbol{\omega}}\hat{\boldsymbol{A}}_1\tilde{\boldsymbol{\omega}}^H}{\tilde{\boldsymbol{\omega}}\hat{\boldsymbol{B}}_1\tilde{\boldsymbol{\omega}}^H} \geq t_m,\ \frac{\tilde{\boldsymbol{\omega}}\hat{\boldsymbol{A}}_2\tilde{\boldsymbol{\omega}}^H}{\tilde{\boldsymbol{\omega}}\hat{\boldsymbol{B}}_2\tilde{\boldsymbol{\omega}}^H} \geq t_m,\ \|\tilde{\boldsymbol{\omega}}\|^2 = 1,$$

which can be solved by using the interior-point algorithm [30].

Because both $\frac{\tilde{\boldsymbol{\omega}}\hat{\boldsymbol{A}}_1\tilde{\boldsymbol{\omega}}^H}{\tilde{\boldsymbol{\omega}}\hat{\boldsymbol{B}}_1\tilde{\boldsymbol{\omega}}^H}$ and $\frac{\tilde{\boldsymbol{\omega}}\hat{\boldsymbol{A}}_2\tilde{\boldsymbol{\omega}}^H}{\tilde{\boldsymbol{\omega}}\hat{\boldsymbol{B}}_2\tilde{\boldsymbol{\omega}}^H}$ are Rayleigh-Ritz ratios, whose maximum values are their principle generalized eigenvalues, respectively. Therefore, the smaller of $\lambda_{\max}(\hat{\boldsymbol{A}}_1, \hat{\boldsymbol{B}}_1)$ and $\lambda_{\max}(\hat{\boldsymbol{A}}_2, \hat{\boldsymbol{B}}_2)$ gives an upper bound to the optimal value of (P-7). Then by applying the corresponding principle eigenvector to the other Rayleigh-Ritz ratio, a lower bound to the optimal value of (P-7) is found, if the result is less than the upper bound. Otherwise the upper bound is the optimal value of (P-7).

The procedure of solving (P-7) is concluded in the modified bi-section search (MBSS) algorithm, where η is the predefined stopping threshold of the bi-section search. Our MBSS algorithm starts with a good initial value computed from the upper and lower bounds given by steps 4–11, which might give the optimal solution directly.

To find the optimal beamformer and power allocation for the multi-relay system, an exhaustive search along the POPA line can be performed, which is described in Algorithm MRO.

Algorithm MRO: Optimal Power Allocation and Beamforming for Multi-Relay systems

1 Quantify $(P_1,\ P_2)$ along the POPA line;
2 For each point $(P_1,\ P_2)$, solve (P-7) by using MBSS, and store the optimal value $t, \boldsymbol{\omega}$;
3 Compare all t's, choose the largest one, and output the corresponding $P_1,\ P_2,\ \boldsymbol{\omega}$ as optimal power allocation and beamforming vector.

IV. Sub-Optimal Beamforming and Power Allocation for Multi-Relay Systems

Because MRO exhaustively searches along the POPA line and employs the nested bi-section search and the interior-point algorithm, its computational complexity is high. Fortunately, the choice of quantization step allows a trade-off between the computational complexity and the achievable SINR. To this end, two low-complexity sub-optimal algorithms (SPA and TPS) are developed in this section.

A. Simple-Power-Allocation (SPA) Algorithm

As mentioned in Section III-B, steps 4–11 in MBSS give a lower bound or even the optimal value to (P-7). Therefore, we can quantify the POPA line, and apply steps 4–11 in MBSS at each power allocation, then choose the power allocation with the highest lower bound to the optimal value of the corresponding problem (P-7) as the sub-optimal power allocation. Finally MBSS is applied to find the sub-optimal $\boldsymbol{\omega}$ corresponding to this sub-optimal power allocation. This approach is named as Simple-Power-Allocation (SPA).

Algorithm SPA: Simple-Power-Allocation Approach

1 Quantify $(P_1,\ P_2)$ along the POPA line;
2 **for** *each pair of* $(P_1,\ P_2)$ **do**
  Steps 1–11 in MBSS algorithm
end
3 Choose $(P_1^{SubOpt}, P_2^{SubOpt})$ with the largest $\min\{t_l, t_u\}$;
4 Solve (P-7) with $(P_1,\ P_2) = (P_1^{SubOpt}, P_2^{SubOpt})$ using MBSS, which returns $\boldsymbol{\omega}^{SubOpt}$;
5 Return $(P_1^{SubOpt}, P_2^{SubOpt})$ and $\boldsymbol{\omega}^{SubOpt}$ as the sub-optimal power allocation and beamformer.

B. Two-Phase Search Algorithm

To further eliminate the exhaustive search, we propose a two-phase search (TPS) algorithm in this section as follows.

Algorithm TPS: Two-Phase Search

1 Compute $(P_1^0,\ P_2^{\max})$ and $(P_1^{\max},\ P_2^0)$, the cross points of $a_1P_1 + a_2P_2 = I_{th}$ with $P_2 = P_2^{\max}$ and $P_1 = P_1^{\max}$, respectively;
2 *Phase I:* Solve (P-10), (P-11) and (P-12) by using combined bi-section search and interior-point algorithm, and choose the one with the largest optimal value, compute the corresponding $(P_1^{SubOpt}, P_2^{SubOpt})$;
3 *Phase II:* Let $(P_1,\ P_2) = (P_1^{SubOpt}, P_2^{SubOpt})$. Solve (P-7) by using MBSS which will return $\boldsymbol{\omega}^{SubOpt}$;
4 Return $(P_1^{SubOpt},\ P_2^{SubOpt})$ and $\boldsymbol{\omega}^{SubOpt}$ as the sub-optimal power allocation and beamformer.

1) Phase I: Sub-Optimal Power Allocation Search: We first decompose the beamforming vector as $\boldsymbol{\omega} \triangleq \sqrt{p}\tilde{\boldsymbol{\omega}}$, where $\|\tilde{\boldsymbol{\omega}}\|^2 = 1$. According to the SINR balancing property, we have $p = [P_2\hat{\sigma_2^2} - P_1\hat{\sigma_1^2}]/[\tilde{\boldsymbol{\omega}}[P_1(\boldsymbol{B}_1 + \boldsymbol{B}_{N_1}) - P_2(\boldsymbol{B}_2 + \boldsymbol{B}_{N_2})]\tilde{\boldsymbol{\omega}}^H]$. Therefore, the optimization problem can be reformulated as

$$\text{(P-9)} \quad \max_{P_1,\,P_2,\,\tilde{\boldsymbol{\omega}}} \ \frac{\tilde{\boldsymbol{\omega}}\boldsymbol{A}\tilde{\boldsymbol{\omega}}^H(P_2\hat{\sigma_2^2} - P_1\hat{\sigma_1^2})}{\tilde{\boldsymbol{\omega}}[\hat{\sigma_2^2}(\boldsymbol{B}_1 + \boldsymbol{B}_{N_1}) - \hat{\sigma_1^2}(\boldsymbol{B}_2 + \boldsymbol{B}_{N_2})]\tilde{\boldsymbol{\omega}}^H}$$

$$\text{s.t.} \quad \|\tilde{\boldsymbol{\omega}}\|^2 = 1,\ p > 0, \tag{17a}$$

$$\Phi(P_1,\ P_2, \tilde{\boldsymbol{\omega}}) = 0, \tag{17b}$$

$$a_1P_1 + a_2P_2 \leq I_{th}, \tag{17c}$$

$$P_1 \leq P_1^{\max}, P_2 \leq P_2^{\max}. \tag{17d}$$

$$\Phi(P_1,\ P_2, \tilde{\boldsymbol{\omega}}) = k_1P_2^2 + k_2P_1P_2 + k_3P_1^2 + k_4P_2 + k_5P_1,$$

$$\text{where } k_1 = \hat{\sigma_2^2}\tilde{\boldsymbol{\omega}}\boldsymbol{C}_2\tilde{\boldsymbol{\omega}}^H,$$

$$k_2 = \hat{\sigma_2^2}\tilde{\boldsymbol{\omega}}\boldsymbol{C}_1\tilde{\boldsymbol{\omega}} - \hat{\sigma_1^2}\tilde{\boldsymbol{\omega}}\boldsymbol{C}_2\tilde{\boldsymbol{\omega}}^H,$$

$$k_3 = -\hat{\sigma_1^2}\tilde{\boldsymbol{\omega}}\boldsymbol{C}_1\tilde{\boldsymbol{\omega}}^H,$$

$$k_4 = \hat{\sigma_2^2}\tilde{\boldsymbol{\omega}}\boldsymbol{C}_3\tilde{\boldsymbol{\omega}} + I_{th}\tilde{\boldsymbol{\omega}}(\boldsymbol{B}_2 + \boldsymbol{B}_{N2})\tilde{\boldsymbol{\omega}}^H,$$

$$k_5 = -\hat{\sigma_1^2}\tilde{\boldsymbol{\omega}}\boldsymbol{C}_3\tilde{\boldsymbol{\omega}}^H - I_{th}\tilde{\boldsymbol{\omega}}(\boldsymbol{B}_1 + \boldsymbol{B}_{N1})\tilde{\boldsymbol{\omega}}^H. \tag{18}$$

With fixed $\tilde{\boldsymbol{\omega}}$, the equality constraint (17b) becomes a hyperbolic curve $\Phi(P_1,\ P_2) = 0$ passing $(0,\ 0)$. Sim-

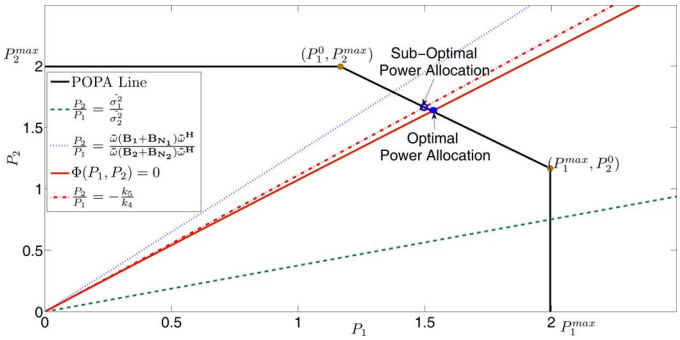

Fig. 4. An Example of TPS Phase I for Multi-Relay Cognitive System with $\tilde{\boldsymbol{\omega}}[\hat{\sigma_2^2}(\boldsymbol{B}_1+\boldsymbol{B}_{N_1})-\hat{\sigma_1^2}(\boldsymbol{B}_2+\boldsymbol{B}_{N2})]\tilde{\boldsymbol{\omega}}^H>0$.

ilar to the analysis in the single-relay case, in order to keep both SINR and p positive, (P_1, P_2) must be chosen such that P_2/P_1 is in the range between $\hat{\sigma_1^2}/\hat{\sigma_2^2}$ and $[\tilde{\boldsymbol{\omega}}(\boldsymbol{B}_1+\boldsymbol{B}_{N_1})\tilde{\boldsymbol{\omega}}^H]/[\tilde{\boldsymbol{\omega}}(\boldsymbol{B}_2+\boldsymbol{B}_{N_2})\tilde{\boldsymbol{\omega}}^H]$. Indeed, $\Phi(P_1,\,P_2)=0$ is always inside this range. As a result, with fixed $\tilde{\boldsymbol{\omega}}$, the optimal value of (P-9) is achieved at the crosspoint of $\Phi(P_1,\,P_2)=0$ and the POPA line. However, the crosspoint is a complicated function with respect to $\tilde{\boldsymbol{\omega}}$. Therefore, we use the first-order Taylor series around point $(0,0)$ to approximate the original hyperbolic curve $\Phi(P_1,\,P_2)=0$ in the first phase. This approximation gives

$$P_2=\left.\frac{\partial\Phi(P_1,\,P_2)}{\partial P_1}\right|_{(P_1=0,P_2=0)}P_1=\frac{-k_5}{k_4}P_1. \tag{19}$$

Replacing (17b) with (19), the optimal power allocation to (P-9) with fixed $\tilde{\boldsymbol{\omega}}$ is the crosspoint of (19) and the POPA line. As the POPA line must be one of the five cases shown in Fig. 2, we use the most complicated case (case (d)), shown in Fig. 4, as an example, where the POPA line has three parts. For each part, we can reformulate (P-9) as a new optimization problem.

PART 1: from $(0, P_2^{\max})$ to $(P_1^0, P_2^{\max})$

$$\text{(P-10)}\quad \max_{\tilde{\boldsymbol{\omega}}}\quad I_{th}P_2^{\max}\frac{\tilde{\boldsymbol{\omega}}\boldsymbol{A}\tilde{\boldsymbol{\omega}}^H}{\tilde{\boldsymbol{\omega}}[\hat{\sigma_1^2}\boldsymbol{C}_3+I_{th}(\boldsymbol{B}_1+\boldsymbol{B}_{N_1})]\tilde{\boldsymbol{\omega}}^H}$$
$$\text{s.t.}\quad P_2^{\max}\frac{\tilde{\boldsymbol{\omega}}[\hat{\sigma_2^2}\boldsymbol{C}_3+I_{th}(\boldsymbol{B}_2+\boldsymbol{B}_{N_2})]\tilde{\boldsymbol{\omega}}^H}{\tilde{\boldsymbol{\omega}}[\hat{\sigma_1^2}\boldsymbol{C}_3+I_{th}(\boldsymbol{B}_1+\boldsymbol{B}_{N_1})]\tilde{\boldsymbol{\omega}}^H}<P_1^0.$$

PART 2: line $a_1P_1+a_2P_2=I_{th}$ with P_1 from P_1^0 to $P_1^{\max}$

$$\text{(P-11)}\quad \max_{\tilde{\boldsymbol{\omega}}}\quad f(\tilde{\boldsymbol{\omega}})$$
$$\text{s.t.}\quad P_1^0<f_1(\tilde{\boldsymbol{\omega}})<P_1^{\max},$$

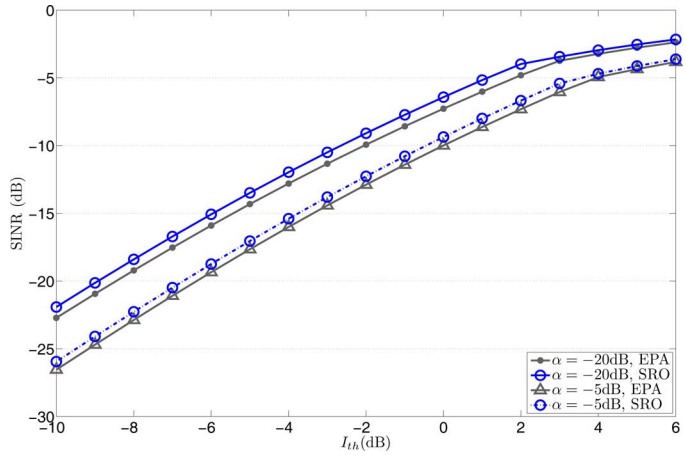

Fig. 5. SINR v.s. I_{th} in a Single-Relay System.

where $f(\tilde{\boldsymbol{\omega}})$ and $f_1(\tilde{\boldsymbol{\omega}})$ are given in (20a) and (20b) at the bottom of the page.

PART 3: from $(P_1^{\max}, P_2^0)$ to $(P_1^{\max}, 0)$

$$\text{(P-12)}\quad \max_{\tilde{\boldsymbol{\omega}}}\quad I_{th}P_1^{\max}\frac{\tilde{\boldsymbol{\omega}}\boldsymbol{A}\tilde{\boldsymbol{\omega}}^H}{\tilde{\boldsymbol{\omega}}[\hat{\sigma_2^2}\boldsymbol{C}_3+I_{th}(\boldsymbol{B}_2+\boldsymbol{B}_{N_2}))]\tilde{\boldsymbol{\omega}}^H}$$
$$\text{s.t.}\quad \frac{\tilde{\boldsymbol{\omega}}[\hat{\sigma_2^2}\boldsymbol{C}_3+I_{th}(\boldsymbol{B}_2+\boldsymbol{B}_{N_2})]\tilde{\boldsymbol{\omega}}^H}{\tilde{\boldsymbol{\omega}}[\hat{\sigma_1^2}\boldsymbol{C}_3+I_{th}(\boldsymbol{B}_1+\boldsymbol{B}_{N_1})]\tilde{\boldsymbol{\omega}}^H}P_1^{\max}<P_2^0.$$

It is obvious that all the fractions in (P-10), (P-11) and (P-12) are Rayleigh-Ritz ratios. Therefore, the nested bi-section search and interior-point algorithm can be employed to solve these problems.

After solving (P-10), (P-11) and (P-12), we choose the one with the largest optimal value and use the corresponding beamforming vector $\tilde{\boldsymbol{\omega}}$ to compute the crosspoint of (19) and the POPA line. This crosspoint is used as the sub-optimal power allocation $(P_1^{SubOpt}, P_2^{SubOpt})$.

2) Phase II: Sub-Optimal Beamforming Vector Search: With $(P_1,\,P_2)=(P_1^{SubOpt}, P_2^{SubOpt})$, we can solve (P-7) by using the MBSS algorithm to obtain the sub-optimal beamformer.

C. Complexity Comparison

In the bi-section search algorithm, the worst-case total number of search points is given as $\log_2\left(\frac{t_u-t_l}{\eta}\right)$, where η is the stopping threshold, and $[t_l,\,t_u]$ is the searching interval. At each search point, we apply the interior-point algorithm to find the optimal solution, which requires running time of $\mathcal{O}(K^{4.5})$ [33]. Because an exhaustive search is employed in both MRO and SPA, we use N to denote the total number of

$$f(\tilde{\boldsymbol{\omega}})=\frac{I_{th}^2\tilde{\boldsymbol{\omega}}\boldsymbol{A}\tilde{\boldsymbol{\omega}}^H}{\tilde{\boldsymbol{\omega}}[a_1(\hat{\sigma_2^2}\boldsymbol{C}_3+I_{th}(\boldsymbol{B}_2+\boldsymbol{B}_{N_2}))+a_2(\hat{\sigma_1^2}\boldsymbol{C}_3+I_{th}(\boldsymbol{B}_1+\boldsymbol{B}_{N_1})]\tilde{\boldsymbol{\omega}}^H} \tag{20a}$$

$$f_1(\tilde{\boldsymbol{\omega}})=\frac{\tilde{\boldsymbol{\omega}}[\hat{\sigma_2^2}\boldsymbol{C}_3+I_{th}(\boldsymbol{B}_2+\boldsymbol{B}_{N_2})]\tilde{\boldsymbol{\omega}}^H}{\tilde{\boldsymbol{\omega}}[a_1(\hat{\sigma_2^2}\boldsymbol{C}_3+I_{th}(\boldsymbol{B}_2+\boldsymbol{B}_{N_2}))+a_2(\hat{\sigma_1^2}\boldsymbol{C}_3+I_{th}(\boldsymbol{B}_1+\boldsymbol{B}_{N_1})]\tilde{\boldsymbol{\omega}}^H}I_{th} \tag{20b}$$

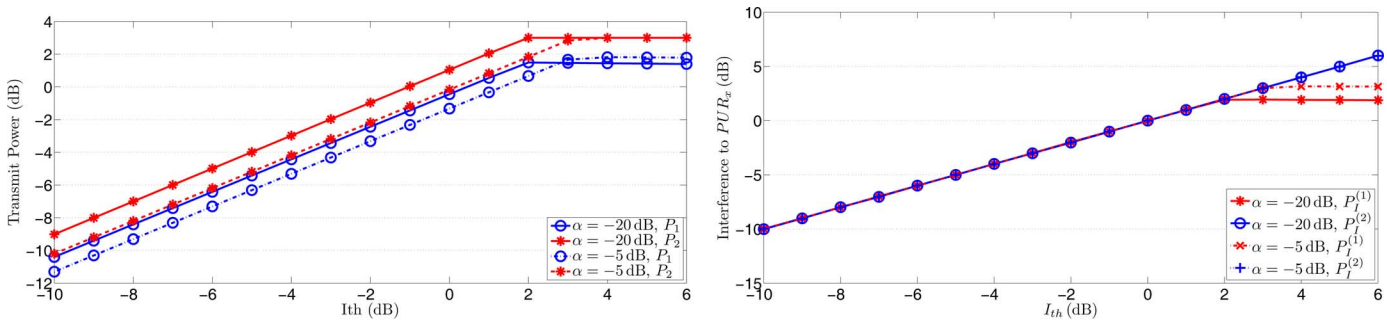

Fig. 6. Optimal Power Allocation and Interference in a Single-Relay System. (a) Transmit Power v.s. I_{th}. (b) Interference v.s. I_{th}.

quantization power allocations (P_1, P_2). Besides, the running time of computing the generalized eigenvalues of two $K \times K$ matrices is $\mathcal{O}(K^3)$. Consequently, the MRO running time is $\mathcal{O}\left(N\left(K^3 + \log_2\left(\frac{t_u - t_l}{\eta}\right)(K^{4.5})\right)\right)$.

Although SPA also performs exhaustive search along the POPA line, at each power allocation only the generalized eigenvalues of the two Rayleigh-Ritz ratios are computed. In addition, only single nested bi-section search execution and interior-point algorithm occurs in the entire process. Therefore, the SPA running time is $\mathcal{O}\left(NK^3 + \log_2\left(\frac{t_u - t_l}{\eta}\right)(K^{4.5})\right)$. Unlike MRO and SPA, TPS allocates sub-optimal power directly by using an approximation process, and requires at most four executions of the nested bi-section search and interior-point algorithm. Accordingly, the TPS running time is $\mathcal{O}\left(4\left(K^3 + \log_2\left(\frac{t_u - t_l}{\eta}\right)(K^{4.5})\right)\right)$. Because both of TPS and SPA reduce the impact of N on the total running time, the computational complexity is reduced dramatically by using either of the two sub-optimal algorithms. For example, if N takes value of 100, both TPS and SPA can reduce over 90% running time, compared with the optimal method.

V. Numerical Results

The optimal and sub-optimal methods are evaluated and compared here. We assume that wireless channels are independent Rayleigh flat fading and generated via the method used in [27], as

$$f = \sqrt{\frac{1}{1+\alpha}}\bar{f} + \sqrt{\frac{\alpha}{1+\alpha}}\tilde{f}, \tag{21}$$

where $\bar{f} \sim \mathcal{CN}(0,1)$ and $\tilde{f} \sim \mathcal{CN}(0,1)$ are the mean and variable components of the complex channel gain, respectively. The mean $\bar{f}$ is generated only once per simulation run. Accordingly, the uncertainty variable α describes the variation of the channel gain from its mean value. To evaluate the effect of α, we simulate with two different α values, -20 dB and -5 dB. Obviously, with a larger α, the channel fluctuates more severely between samples. Same α value is assumed for all channels in each simulation run. Therefore, their second-order statistics are computed as

$$\mathbb{E}\{\|f\|^2\} = \frac{1}{1+\alpha}(\|\bar{f}\|^2 + \alpha), \tag{22}$$

$$\mathbb{E}\{\boldsymbol{f}\boldsymbol{f}^H\} = \frac{1}{1+\alpha}(\bar{\boldsymbol{f}}\bar{\boldsymbol{f}}^H + \alpha I). \tag{23}$$

To further study the impact of the number of relays, we generate three systems with 1, 10 and 20 relays. We further assume that all AWGN components follow $\mathcal{CN}(0,1)$ distribution, and $P_p = P_1^{\max} = P_2^{\max} = 3$ dBm. The (P_1, P_2) trajectory in MRO is quantified with a step size of 0.001.

It is critically important to show the performance gain achieved by our proposed algorithms, compared to a system with equal power allocation and simple AF relaying. We label this benchmark system as EPA. EPA allocates equal powers to the two secondary transceivers, and restricts each relay interference under the threshold given by I_{th}/K. In EPA, the ith relay computes its relaying coefficient as $\omega_i = \frac{I_{th}}{K\mathbb{E}\{\|h_{r_i}\|^2\}}$.

A. Single-Relay System

The SINR v.s. I_{th} curves with two different α values are shown in Fig. 5, where a higher SINR can be achieved with a more stable channel, say $\alpha = -20$ dB, compared with $\alpha = -5$ dB. This result is reasonable because besides $\boldsymbol{g}_j$, SU_j knows only the SOS of other channels.

In addition, a constant SINR gap between $\alpha = -20$ dB and $\alpha = -5$ dB exists when I_{th} is lower than 2 dB. Since I_{th} has increased to 2 dB, the $\alpha = -5$ dB curve converges to the $\alpha = -20$ dB curve, which stays flat. This result occurs because the increase of I_{th} moves the limitation of the power allocation from the constraint on $P_I^{(1)}$ to its maximum value $P^{\max}$, as shown in Fig. 6(a) and (b).

In Fig. 5, the relatively low optimal SINR achieved in the single-relay system is not surprising because the SRO beamforming coefficient is real, so that the phase distortions due to wireless channels have not been mitigated. Thus, system performance is mainly determined by power allocation. Consequently, the relays' capability to improve the system performance is limited, less than 1 dB compared to those with EPA.

B. Multi-Relay System

Figs. 7 – 9 compare MRO, SPA, TPS, and EPA with different α values in 10-relay and 20-relay systems from the SINR and power allocation perspectives, respectively.

As shown in Fig. 7, just like the single-relay case, a higher SINR is synonymous with more stable channels, such as $\alpha = -20$ dB. Unlike the single-relay systems, the phase distortions

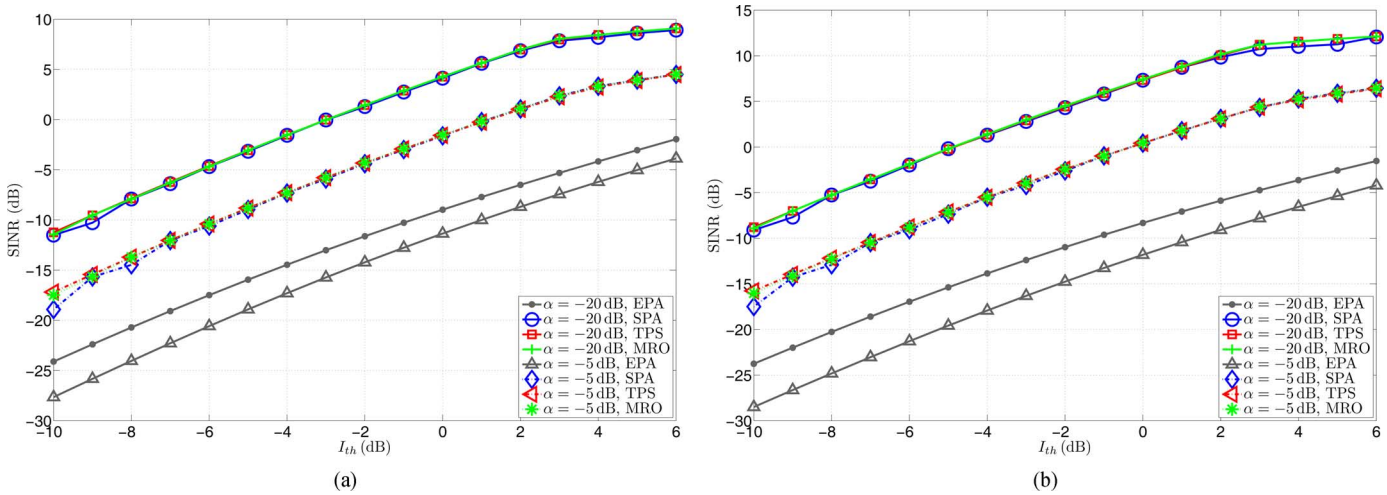

Fig. 7. SINR Comparison of MRO, SPA and TPS. (a) SINR v.s. I_{th} in 10-relay system. (b) SINR v.s. I_{th} in 20-relay system.

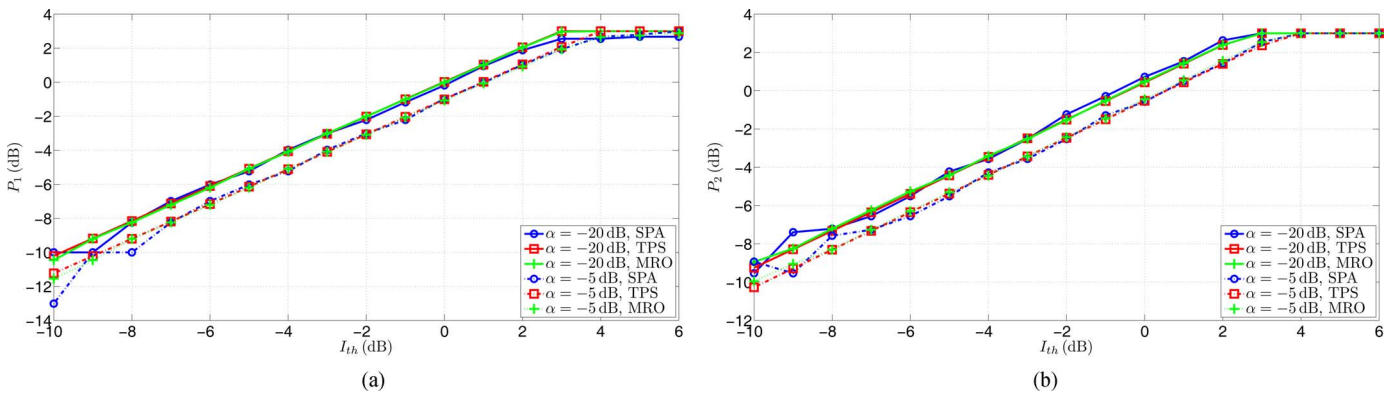

Fig. 8. Power Allocation Comparison of MRO, SPA and TPS in a 10-relay System. (a) P_1 v.s. I_{th}. (b) P_2 v.s. I_{th}.

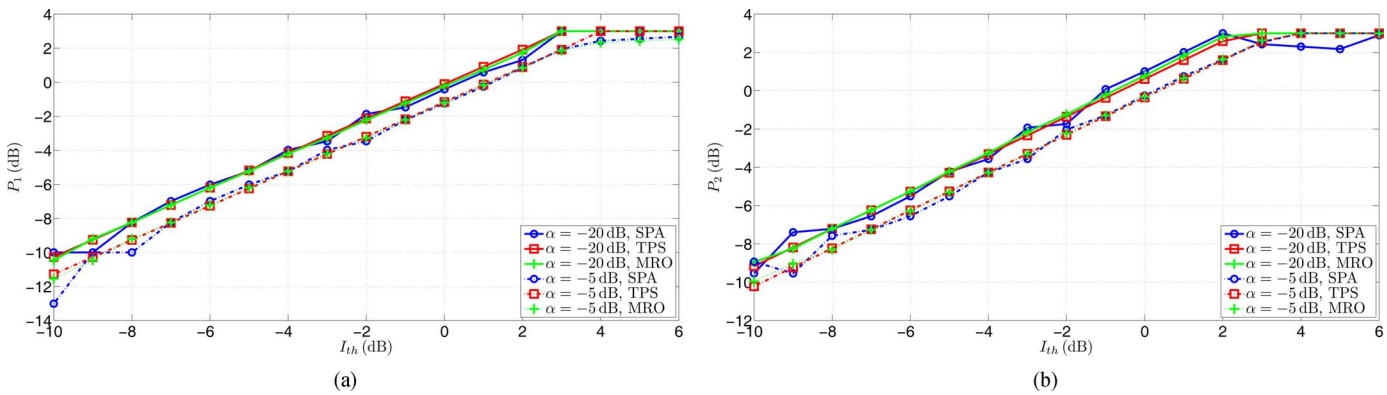

Fig. 9. Power Allocation Comparison of MRO, SPA and TPS in a 20-relay System. (a) P_1 v.s. I_{th}. (b) P_2 v.s. I_{th}.

are compensated for by the MRO beamforming vector. Consequently, joint distributed beamforming and power allocation dramatically improves SINR, e.g., over 10 dB more than EPA. Additionally, Fig. 7 indicates that more relays facilitating the communication achieves higher SINRs. However, the number of relays only mildly affects the optimal power allocation (see Figs. 8 and 9). The reason is that the interference limit $P_I^{(1)}$, which is unrelated to the number of relays, significantly impacts power allocation.

When comparing SPA with MRO, Fig. 7 shows that their SINR gap is less than 0.8 dB and 1.5 dB with $\alpha = -20$ dB and $\alpha = -5$ dB, respectively. Moreover, the SPA power allocations have larger differences when $\alpha = -5$ dB, as shown in Figs. 8 and 9. These differences are due to sub-optimal SPA power allocations. Indeed, the true optimal solution might have a slightly lower lower bound.

Unlike SPA, TPS achieves SINRs closer to the optimal values, with SINR gap less than 0.12 dB. Moreover, TPS even

provides almost the same power allocation as MRO, as shown in Figs. 8 and 9.

VI. Conclusion

This paper has investigated joint distributed beamforming and power allocation to balance and maximize SINR of two secondary transceivers, while taking into consideration all relevant interference constraints. While a closed-form solution is developed for single-relay systems, one optimal and two low-complexity sub-optimal algorithms are proposed for multi-relay systems, where the SINR can be improved dramatically, as high as 10 dB.

Appendix A
Proof of Lemma 1

Assume $(P_1^{opt},\, P_2^{opt},\, \boldsymbol{\omega}^{opt})$ is one optimal solution to (P-1) and $\mathrm{SINR}_1^{opt} \neq \mathrm{SINR}_2^{opt}$. Without loss of generality, we assume that $\mathrm{SINR}_1^{opt} > \mathrm{SINR}_2^{opt}$.

Define $\kappa \triangleq \frac{\mathrm{SINR}_2^{opt}}{\mathrm{SINR}_1^{opt}}$ which satisfies $\kappa < 1$. If we reduce P_2^{opt} to $\tilde{P}_2 \triangleq \kappa P_2^{opt}$, it is obvious that $(P_1^{opt},\, \tilde{P}_2,\, \boldsymbol{\omega}^{opt})$ is also a feasible solution to (P-1) and

$$\widetilde{\mathrm{SINR}}_1 = \kappa \frac{P_2^{opt}\boldsymbol{\omega}^{opt}\boldsymbol{A}(\boldsymbol{\omega}^{opt})^H}{\boldsymbol{\omega}^{opt}(\boldsymbol{B}_1 + \boldsymbol{B}_{N_1})(\boldsymbol{\omega}^{opt})^H + \hat{\sigma_1^2}} = \mathrm{SINR}_2^{opt}.$$

Therefore, $(P_1^{opt},\, \tilde{P}_2,\, \boldsymbol{\omega}^{opt})$ is another optimal solution.

Appendix B
Proof of Lemma 2

Assume $(P_1^{opt},\, P_2^{opt},\, \boldsymbol{\omega}^{opt})$ is an optimal solution to (P-1) with the optimal value SINR^{opt}. Further assume that (8b) and (8c) are satisfied with inequality, $a_1P_1^{opt} + a_2P_2^{opt} < I_{th}$, $P_1^{opt} < P_1^{\max}$, and $P_2^{opt} < P_2^{\max}$.

Define $\kappa \triangleq \min\left\{\frac{P_1^{\max}}{P_1^{opt}},\, \frac{P_2^{\max}}{P_2^{opt}},\, \frac{I_{th}}{a_1P_1^{opt}+a_2P_2^{opt}}\right\}$ which satisfies $\kappa > 1$. Next, we define

$$\tilde{P}_1 \triangleq \kappa P_1^{opt},\ \tilde{P}_2 \triangleq \kappa P_2^{opt},\ \tilde{\boldsymbol{\omega}} \triangleq \frac{1}{\sqrt{\kappa}}\boldsymbol{\omega}^{opt}.$$

$(\tilde{P}_1, \tilde{P}_2, \tilde{\boldsymbol{\omega}})$ is also a feasible point of (P-1) and $\min\{\mathrm{SINR}_1(\tilde{P}_2, \tilde{\boldsymbol{\omega}}), \mathrm{SINR}_2(\tilde{P}_1, \tilde{\boldsymbol{\omega}})\} > \mathrm{SINR}^{opt}$, which contradicts with that $(P_1^{opt},\, P_2^{opt},\, \boldsymbol{\omega}^{opt})$ is an optimal solution to (P-1). Therefore, at least one of the three inequalities in (8b) and (8c) should be satisfied with equality at the optimal point.

Appendix C
Proof of Lemma 3

Assume $(P_1^{opt},\, P_2^{opt},\, \boldsymbol{\omega}^{opt})$ is an optimal solution to (P-1) with the optimal value SINR^{opt}. Further, we assume that (8a) is satisfied with inequality.

Define $\kappa \triangleq I_{th}/[\boldsymbol{\omega}^{opt}(P_1^{opt}\boldsymbol{C}_1 + P_2^{opt}\boldsymbol{C}_2 + \boldsymbol{C}_3)(\boldsymbol{\omega}^{opt})^H]$, which is obviously larger than one. Then define a new beamforming vector $\tilde{\boldsymbol{\omega}} \triangleq \sqrt{\kappa}\boldsymbol{\omega}^{opt}$. $(P_1^{opt},\, P_2^{opt},\, \tilde{\boldsymbol{\omega}})$ also satisfies the constraints (8b) and (8c). And the constraint (8a) is satisfied with equality. We even have

$$\mathrm{SINR}_1(P_2^{opt}, \tilde{\boldsymbol{\omega}}) > \mathrm{SINR}_1(P_2^{opt}, \boldsymbol{\omega}^{opt}),$$
$$\mathrm{SINR}_2(P_1^{opt}, \tilde{\boldsymbol{\omega}}) > \mathrm{SINR}_2(P_1^{opt}, \boldsymbol{\omega}^{opt}),$$

which contradicts with that $(P_1^{opt},\, P_2^{opt},\, \boldsymbol{\omega}^{opt})$ is an optimal solution to (P-1).

References

[1] Federal Communications Commission, "Spectrum Policy Task Force," Rep. ET Docket, Tech. Rep. 02-135, Nov. 2002.

[2] Q. Zhao and B. Sadler, "A survey of dynamic spectrum access," *IEEE Signal Process. Mag.*, vol. 24, no. 3, pp. 79–89, May 2007.

[3] B. Wang and K. Liu, "Advances in cognitive radio networks: A survey," *IEEE J. Sel. Topics Signal Process.*, vol. 5, no. 1, pp. 5–23, Feb. 2011.

[4] S. Haykin, "Cognitive radio: Brain-empowered wireless communications," *IEEE J. Sel. Areas Commun.*, vol. 23, no. 2, pp. 201–220, Feb. 2005.

[5] A. Goldsmith, S. Jafar, I. Maric, and S. Srinivasa, "Breaking spectrum gridlock with cognitive radios: An information theoretic perspective," *Proc. IEEE*, vol. 97, no. 5, pp. 894–914, May 2009.

[6] B. Rankov and A. Wittneben, "Spectral efficient protocols for half-duplex fading relay channels," *IEEE J. Sel. Areas Commun.*, vol. 25, no. 2, pp. 379–389, Feb. 2007.

[7] A. Sendonaris, E. Erkip, and B. Aazhang, "User cooperation diversity–Part I. System description," *IEEE Trans. Commun.*, vol. 51, pp. 1927–1938, Nov. 2003.

[8] A. Sendonaris, E. Erkip, and B. Aazhang, "User cooperation diversity–Part II. Implementation aspects and performance analysis," *IEEE Trans. Commun.*, vol. 51, pp. 1939–1948, Nov. 2003.

[9] J. Laneman, D. Tse, and G. Wornell, "Cooperative diversity in wireless networks: Efficient protocols and outage behavior," *IEEE Trans. Inf. Theory*, vol. 50, pp. 3062–3080, Dec. 2004.

[10] A. Molisch, *Wireless Communication*. New York, NY, USA: Wiley-IEEE, 2005.

[11] S. Safavi, M. Ardebilipour, R. Zadeh, and A. Piltan, "SINR balancing approach for network beamforming in cognitive two-way relay networks," in *Proc. 11th Int. Conf. Hybrid Intell. Syst.*, Dec. 2011, pp. 481–485.

[12] G. Amarasuriya, C. Tellambura, and M. Ardakani, "Joint beamforming and antenna selection for two-way amplify-and-forward MIMO relay networks," in *Proc. IEEE Int. Conf. Commun.(ICC)*, Dec. 2012, pp. 4829–4834.

[13] H. Bagheri, M. Ardakani, and C. Tellambura, "Resource allocation for two-way AF relaying with receive channel knowledge," *IEEE Trans. Wireless Commun.*, vol. 11, no. 6, pp. 2002–2007, Jun. 2012.

[14] G. Amarasuriya, C. Tellambura, and M. Ardakani, "Performance analysis of zero-forcing for two-way MIMO AF relay networks," *IEEE Wireless Commun. Lett.*, vol. 1, no. 2, pp. 53–56, Apr. 2012.

[15] S. ShahbazPanahi and M. Dong, "A semi-closed-form solution to optimal distributed beamforming for two-way relay networks," *IEEE Trans. Signal Process.*, vol. 60, pp. 1511–1516, Mar. 2012.

[16] S. Shahbazpanahi and M. Dong, "Achievable rate region under joint distributed beamforming and power allocation for two-way relay networks," *IEEE Trans. Wireless Commun.*, vol. 11, pp. 4026–4037, Nov. 2012.

[17] V. Havary-Nassab, S. ShahbazPanahi, and A. Grami, "Optimal distributed beamforming for two-way relay networks," *IEEE Trans. Signal Process.*, vol. 58, pp. 1238–1250, Mar. 2010.

[18] S. ShahbazPanahi and M. Dong, "A semi-closed form solution to the SNR balancing problem of two-way relay network beamforming," in *Proc. IEEE Int. Conf. Acoust., Speech Signal Process. (ICASSP)*, Mar. 2010, pp. 2514–2517.

[19] Y. Jing and S. ShahbazPanahi, "Max-min optimal joint power control and distributed beamforming for two-way relay networks under per-node power constraints," *IEEE Trans. Signal Process.*, vol. 60, pp. 6576–6589, Dec. 2012.

[20] K. Hamdi, M. Hasna, A. Ghrayeb, and K. Letaief, "Priority-based zero-forcing in spectrum sharing cognitive systems," *IEEE Commun. Lett.*, vol. 17, no. 2, pp. 313–316, Feb. 2013.

[21] S. Song, M. Hasna, and K. Letaief, "Prior zero forcing for cognitive relaying," *IEEE Trans. Wireless Commun.*, vol. 12, no. 2, pp. 938–947, Feb. 2013.
[22] J. Tang and S. Lambotharan, "Beamforming and temporal power optimisation for an overlay cognitive radio relay network," *IET Signal Process.*, vol. 5, no. 6, pp. 582–588, 2011.
[23] Z. Dai, J. Liu, C. Wang, and K. Long, "An adaptive cooperation communication strategy for enhanced opportunistic spectrum access in cognitive radios," *IEEE Commun. Lett.*, vol. 16, no. 1, pp. 40–43, Jul. 2012.
[24] J. Liu, W. Chen, Z. Cao, and Y. Zhang, "Cooperative beamforming for cognitive radio networks: A cross-layer design," *IEEE Trans. Commun.*, vol. 60, no. 5, pp. 1420–1431, May 2012.
[25] T. Luan, F. Gao, X.-D. Zhang, J. Li, and M. Lei, "Rate maximization and beamforming design for relay-aided multiuser cognitive networks," *IEEE Trans. Veh. Technol.*, vol. 61, no. 4, pp. 1940–1945, May 2012.
[26] Q. Li, Q. Zhang, R. Feng, L. Luo, and J. Qin, "Optimal relay selection and beamforming in MIMO cognitive multi-relay networks," *IEEE Commun. Lett.*, vol. 17, no. 6, pp. 1188–1191, Jun. 2013.
[27] A. Piltan and S. Salari, "Distributed beamforming in cognitive relay networks with partial channel state information," *IET Commun.*, vol. 6, pp. 1011–1018, Jan. 2012.
[28] S. Safavi, M. Ardebilipour, V. Jamali, and M. Ahmadian, "Distributed beamforming for SINR balancing approach in cognitive two-way relay networks with imperfect channel state information," in *Proc. 20th Iranian Conf. Elect. Eng.*, May 2012, pp. 1342–1346.
[29] S. Safavi, M. Ardebilipour, and S. Salari, "Relay beamforming in cognitive two-way networks with imperfect channel state information," *IEEE Wireless Commun. Lett.*, vol. 1, no. 4, pp. 344–347, Aug. 2012.
[30] S. Boyd and L. Vandenberghe, *Convex Optimization*. Cambridge, U.K.: Cambridge Univ. Press, 2004.
[31] G. Wang, F. Gao, W. Chen, and C. Tellambura, "Channel estimation and training design for two-way relay networks in time-selective fading environments," *IEEE Trans. Wireless Commun.*, vol. 10, no. 8, pp. 2681–2691, Aug. 2011.
[32] C. Li, L. Yang, and W.-P. Zhu, "Robust distributed beamforming for two-way wireless relay systems," in *Proc. IEEE Int. Symp. Circuits Syst. (ISCAS)*, 2010, pp. 3108–3111.
[33] Z.-Q. Luo, W.-K. Ma, A.-C. So, Y. Ye, and S. Zhang, "Semidefinite relaxation of quadratic optimization problems," *IEEE Signal Process. Mag.*, vol. 27, no. 3, pp. 20–34, May 2010.

Yun Cao received the B.Sc. degree in automation from Southeast University, China, in 2007 and the M.Eng. degree in automation from Southeast University, China, in 2010.

She is currently working towards the Ph.D. degree in electrical and computer engineering at the University of Alberta, Edmonton, Alberta, Canada. Her research interests include beamforming and power allocation in cooperative cognitive relay networks, and performance analysis in cognitive networks.

Chintha Tellambura (F'11) received the B.Sc. degree (with first-class honor) from the University of Moratuwa, Sri Lanka, in 1986, the M.Sc. degree in Electronics from the University of London, U.K., in 1988, and the Ph.D. degree in Electrical Engineering from the University of Victoria, Canada, in 1993.

He was a Postdoctoral Research Fellow with the University of Victoria (1993–1994) and the University of Bradford (1995–1996). He was with Monash University, Australia, from 1997 to 2002. Presently, he is a Professor with the Department of Electrical and Computer Engineering, University of Alberta. His research interests focus on communication theory dealing with the wireless physical layer.

Prof. Tellambura is an Associated Editor for the IEEE TRANSACTIONS ON COMMUNICATION and the Area Editor for Wireless Communications Systems and Theory in the IEEE TRANSACTIONS ON WIRELESS COMMUNICATIONS. He was Chair of the Communication Theory Symposium in Globecom'05 held in St. Louis, MO.